A Transforming Growth Factor-α–*Pseudomonas* Exotoxin Hybrid Protein Undergoes pH-Dependent Conformational Changes Conducive to Membrane Interaction

Gautam Sanyal,* Dorothy Marquis-Omer,* Jacqueline O'Brien Gress, and C. Russell Middaugh

Department of Pharmaceutical Research, WP 26-331, Merck Research Laboratories, West Point, Pennsylvania 19486

Received November 13, 1992; Revised Manuscript Received January 29, 1993

ABSTRACT: TP40 is a chimeric protein containing transforming growth factor α (TGF-α) at the N-terminus and a derivative of a 40 000-Da segment (PE40δcys) of *Pseudomonas* exotoxin (PE). PE40δcys contains domains Ib, II, and III of PE in which the cysteines are mutated to alanines. The rationale for inclusion of TGF-α is to provide TP40 with selective targeting toward cells expressing the epidermal growth factor receptor (EGFr) on their surface [Pastan, I., & FitzGerald, D. (1989) *J. Biol. Chem. 264*, 15157–15160]. Translocation across endosomal membranes is thought to be a required step for cytotoxic activity of PE. This step is presumably facilitated by the low pH in endosomes which induces exposure of a hydrophobic surface of the protein, which in turn becomes available to interact with and translocate across the membrane. We have employed the hydrophobic fluorescence probe 2-*p*-toludinylnaphthalene-6-sulfonate (TNS) and the intrinsic tryptophan fluorophores of TP40 to investigate pH-induced changes in the tertiary structure of this protein. The pH dependence of TP40 interaction with liposomes also provided a model for studying protein–membrane interactions. TNS fluorescence was markedly enhanced in the presence of TP40 below pH 4 and to a lesser degree between pH 7 and 5. A progressive red shift of tryptophan fluorescence with decreasing pH was also seen with the approximate midpoint for this transition occurring around pH 3. Both observations suggest that acidic pH induces exposure of hydrophobic regions of TP40, making them accessible to solvent and TNS. No major alteration of the secondary structure was manifested in the far-UV CD spectrum of TP40 upon a reduction in pH from 7 to 2. Thus, the low-pH-induced structural change of TP40 appears to involve a subtle exposure of one or more hydrophobic surfaces without an extensive unfolding of the protein's secondary structure. In the presence of anionic liposomes, a low-pH-induced blue shift of the TP40 tryptophan fluorescence was observed, suggesting that interaction with liposomes also required the low-pH conformation of the protein. However, the midpoint of this fluorescence blue shift occurred at approximately pH 5, which is presumably closer to the physiological pH within endosomes. Neutral liposomes failed to induce these spectral changes in TP40, implying a lack of interaction with these lipids. At acidic pH values between 2 and 4, self-association of TP40 in solution was detected by equilibrium sedimentation and quasielastic light scattering measurements. This probably results from intermolecular interaction between exposed hydrophobic surfaces. The results presented suggest that TP40 retains the structural characteristics of PE that are required for translocation.

TGF-α–PE40[1] is a chimeric toxin designed to bind to and kill cells expressing high levels of epidermal growth factor receptor (EGFr) (Chaudhury et al., 1987; Edwards et al., 1989; Pastan & FitzGerald, 1989). Exploitation of the elevation in EGFr on certain tumor cell types relative to their nontransformed counterparts has led to the development of this hybrid protein as a potential chemotherapeutic agent (Pastan & FitzGerald, 1991; Pastan et al., 1992). TGF-α–PE40 contains a 40 000-Da segment, PE40, derived from *Pseudomonas aeruginosa* exotoxin A (PE) fused to transforming growth factor α (TGF-α). The cytotoxic mechanism of PE is initiated by cell surface receptor binding and entry into cells via coated pits which subsequently fuse with endosomal vesicles (FitzGerald et al., 1980; Morris et al., 1985). Upon acidification in endosomes by an intrinsic proton pump, one or more hydrophobic regions of the toxin are exposed. The appearance of these hydrophobic surfaces facilitates insertion into the endosomal membrane and translocation into the cytoplasm (Draper & Simon, 1980; Zalman & Wisnieski, 1985; Sandvig & Moskaug, 1987; Farahbakhsh & Wisnieski, 1989; Jiang & London, 1990). Cytotoxicity results from termination of protein synthesis following ADP-ribosylation of elongation factor 2 (EF-2) by the translocated PE (Iglewski & Kabat, 1975). This last step is also the final step in the pathway of cytotoxic action of diphtheria toxin (Collier, 1975). The membrane translocation of diphtheria toxin, like that of PE, is facilitated by the low-pH environment in the endosome which induces exposure of hydrophobic surfaces (Sandvig & Olsnes, 1980; Blewitt et al., 1985; Collins & Collier, 1987).

* Authors to whom correspondence should be addressed. Telephone: (215) 652-3975 (G.S.). Fax: (215) 652-5299.

[1] Abbreviations: PE, *Pseudomonas* exotoxin A; PE40, a 40 000-Da segment of PE; TGF-α, transforming growth factor α; TGF-α–PE40, a chimera of transforming growth factor α and a 40 000-Da segment of *Pseudomonas* exotoxin; ADP, adenosine 5′-diphosphate; EF-2, elongation factor 2; PE40δcys, a mutant of PE40 in which all four cysteine residues are replaced with alanine; EGFr, the epidermal growth factor receptor; GuHCl, guanidine hydrochloride; SDS, sodium dodecyl sulfate; TNS, 2-*p*-toludinylnaphthalene-6-sulfonic acid (or sulfonate); DSPC, distearoylphosphatidylcholine; DOPG, dioleoylphosphatidylglycerol; PC, phosphatidylcholine; REV, reverse evaporation vesicle; MTT, 3-(4,5-dimethylthiazol-2-yl)-2,5-diphenyltetrazolium bromide; PCS, percent cell survival; CD, circular dichroism; τ, lifetime of singlet excited state measured by fluorescence decay; FTIR, Fourier transform infrared spectroscopy; QLS, quasielastic light scattering; rpm, revolutions per minute; ns, nanoseconds.

0006-2960/93/0432-3488$04.00/0

It has been proposed that in the endosome PE is proteolytically clipped to generate a 37-kDa "active" fragment, which is then translocated (Ogata et al., 1990). PE contains three distinct functional molecular regions specific to either cell binding, translocation, or ADP-ribosylation. Three structural domains were observed in the crystal structure of PE resolved to 3 Å (Allured et al., 1986). Domain I is further subdivided into a large domain Ia and a smaller domain Ib, the former being critical for cell binding of PE. Translocation and ADP-ribosylation functions have been attributed to domains II and III, respectively (Pastan & Fitzgerald, 1989). The putative receptor for PE, the α2-macroglobulin receptor/low-density lipoprotein receptor-related protein, is present on the surface of virtually all eukaryotic cells and allow nonspecific PE intoxication (Kounnas et al., 1992). In contrast, TGF-α–PE40, while retaining domains Ib, II, and III of PE, substitutes TGF-α for domain Ia of PE. The high affinity of TGF-α for EGFr (Massague, 1983; Winkler et al., 1986) confers on this chimeric molecule a specificity for EGFr which is overexpressed on the surface of several kinds of tumor cells. Therapeutic selectivity in cell targeting is thereby achieved (Edwards et al., 1989).

The three disulfides of TGF-α are critical for the peptide's binding to EGFr (Marquardt et al., 1984; Lee et al., 1985). Substitution of alanine for the four cysteine residues of PE40, on the other hand, does not abrogate cytotoxic activity. The mutant of TGF-α–PE40 which has alanine substituted for the PE40 cysteines (PE40δcys) is termed TP40 and manifests antitumor activity against xenographic implants in nude mice (Edwards et al., 1989; Heimbrook et al., 1990). Furthermore, it has shown marked in vitro cytotoxic activity against a variety of primary human tumors taken directly from patients and grown in soft agar (Von Hoff et al., 1992). The EGFr binding activity of TP40 was found to be approximately 15-fold greater than that of unmutated TGF-α–PE40 (Edwards et al., 1989). The enhanced EGFr specificity of TP40 compared to TGF-α–PE40 offers the possibility of a wider therapeutic window in chemotherapeutic use. The in vitro A431 cell-kill activity of TP40 is, however, an order of magnitude lower than that of TGF-α–PE40 (Edwards et al., 1989).

In this study we have, therefore, examined whether the structural elements that are believed to be important in translocation of native PE across endosomal membranes have been retained in TP40. More specifically, the effect of acidification on the secondary and tertiary structure of this protein has been studied. The effect of lipid environment on TP40 has been investigated by examining the interaction of TP40 with liposomes which serve as a model of the endosomal membrane. Our data indicate that exposure of hydrophobic surface(s) occurs at acidic pH without a change in the overall secondary structure of the protein. This subtle structural alteration appears to be predominantly localized in the PE40δcys portion of the molecule. These observations support the conclusion that TP40 contains a functional translocation domain and that it is important for the functional activity of the hybrid protein.

METHODS

Proteins. Recombinant TP40 was purified as described (Edwards et al., 1989; Heimbrook et al., 1990). PE40δcys was obtained as a byproduct in the purification process of TP40. The identities of these proteins were confirmed by amino acid sequencing, and their purities were greater than 99% as judged by densitometric scans of Coomassie-stained SDS–polyacrylamide gels.

Protein concentrations were determined spectrophotometrically using extinction coefficients of 45 460 and 43 980 M^{-1} cm^{-1} at 280 nm for TP40 and PE40δcys, respectively. These values were calculated from the protein amino acid compositions using average extinction coefficients of 5540 M^{-1} cm^{-1} for tryptophan and 1480 M^{-1} cm^{-1} for tyrosine residues (Mach et al., 1992). Equivalencies: 1 mg/mL TP40 is 22 μM; 1 mg/mL PE40δcys is 26 μM.

Reagents and Buffer. 2-*p*-Toludinylnaphthalene-6-sulfonic acid (TNS) was purchased from Molecular Probes (Eugene, OR). Human transforming growth factor-α and 3-(4,5-dimethylthiazol-2-yl)-2,5-diphenyltetrazolium bromide (MTT) were obtained from Sigma Chemical Company (St. Louis, MO). Guanidine hydrochloride was a product of BRL (Gaithersburg, MD). Distearoyl and bis(bromostearoyl) phosphatidylcholine (DSPC and brominated DSPC), dioleoylphosphatidylglycerol (DOPG), egg phosphatidylcholine (PC), and cholesterol were obtained from Avanti Polar Lipids (Alabaster, AL) and used as received. All buffer solutions contained, unless indicated otherwise, sodium phosphate at a concentration of 100 mM.

Phospholipid and Liposome Preparation. Reverse evaporation vesicles (REVs) were formed according to published procedures (Szoka & Papajopoulas, 1978). Typically, 100 μmol of lipid was mixed well and dried under vacuum for a minimum of 2 h. The dried film was hydrated in buffer (10 mM sodium phosphate, pH 7.4) to a final lipid concentration of 10 μmol/mL. Resuspension was facilitated by intermittent vortexing. Diethyl ether was added at three times the volume of the lipid suspension, and the mixture was sonicated until a stable emulsion formed. Ether was removed under partial vacuum until a gel formed which was subsequently broken under increasing vacuum. REVs were held at 4 °C until the day of use when they were extruded through 0.2-μm polycarbonate filters or, for CD measurements, two 0.1-μm polycarbonate filters. Liposomes were held on wet ice until use.

Cell-Kill Assays. A431 epithelial carcinoma cells were obtained from the American Type Culture Collection. They were maintained in minimum essential medium (α-medium) supplemented with 10% (v/v) fetal calf serum, antibiotics, and nonessential amino acids. The cell-killing activity of TP40 against these cells was determined by performing the procedure described by Heimbrook et al. (1990). Briefly, MTT (3-(4,5-dimethylthiazol-2-yl)-2,5-diphenyltetrazolium bromide), a dye which detects metabolic activity, is added to TP40-treated and untreated cells. Percent cell survival (PCS) across a TP40 concentration gradient is calculated by dividing the amount of dye uptake in treated cells by the amount of uptake in untreated cells. The TP40 concentration at which PCS is 50% (EC_{50}) is calculated by a four-parameter logistic curve-fitting analysis of the PCS versus TP40 concentration (logarithmic scale) curve.

Circular Dichroism (CD). CD spectra were measured using a JASCO J-720 spectropolarimeter. A cylindrical quartz cuvette of 0.1 mm path length and protein concentrations of 11–22 μM were used for measurements made in aqueous buffer solutions in the absence of lipids. The temperature was controlled with a circulating water bath connected to a jacketed cuvette. Secondary structure analysis was carried out by the variable selection method of Manavalan and Johnson (1987).

All samples containing REVs were filtered through two 0.1-μm polycarbonate filters prior to CD measurements and placed in a quartz cuvette of 1 cm path length. TP40 was added to a diluted liposome suspension, and for measurements at low pH, the pH was adjusted by direct titration with HCl.

Concentrations of TP40 and REVs were 0.24 μM each after mixing. CD spectra were corrected for the background signal arising from light scattering by liposome suspensions in buffer.

Fluorescence Spectra. Steady-state fluorescence spectra were measured with either a SPEX Fluorolog 2 instrument equipped with a double emission monochromator or an ISS GREG2 photon counting spectrofluorometer. TP40 and PE40δcys samples were excited at 280 or 295 nm for measurement of tryptophan fluorescence spectra. Excitation and emission slit widths were 4 and 8 nm, respectively. Spectra were corrected for Raman scatter and for wavelength-dependent monochromator artifacts. Tryptophan fluorescence anisotropy was measured in the ISS GREG2 fluorometer using Glan Thomson polarizers. Samples were excited at 300 nm, and emission was monitored at 350 nm. A *G*-factor correction was employed to compensate for monochromator response. TNS binding to TP40 was monitored by exciting TNS fluorescence at 315 nm and monitoring TNS emission between 400 and 500 nm. Fluorescence intensity at the λ_{max} (430 nm) was used to monitor the effect of pH on TNS fluorescence.

Fluorescence spectra of samples containing REVs were measured at TP40 and liposome concentrations of 0.24 and 1.8 μM, respectively. Spectra were corrected for the background signal from liposome suspensions.

Fluorescence Lifetime. The tryptophan fluorescence lifetime (τ) of TP40 was measured with a modified ISS GREG200 multiple-frequency phase fluorometer equipped with a digital filter for data acquisition through a fast Fourier transform routine. Modulation frequencies ranged from 8 to 120 MHz, and a cross-correlation frequency of 80 Hz was employed. Phase shifts and demodulation ratios were analyzed by multiexponential least-squares analysis (Lakowicz et al., 1984). TP40 solutions, at 1 mg/mL, were excited at 295 nm, and the emitted light was passed through a Shott glass filter that permits transmission above 345 nm. *p*-Terphenyl (τ = 1.05 ns) was used as the reference.

Fourier Transform Infrared (FTIR) Spectroscopy. FTIR spectra were measured with a Digilab FTS-60 spectrometer. A CaF_2 cell of 100 μm path length and an MCT detector were used. TP40 and PE40δcys solutions at concentrations of 4.9 and 6.0 mg/mL, respectively, in D_2O buffered at a pD of 7.2 with 6.2 mM sodium phosphate and 150 mM NaCl were employed. Spectra were partially deconvoluted (Kauppinen et al., 1981) and then fitted to mixed Gaussian/Lorentzian curves using second derivative peak positions as initial queries. Further deconvolution was achieved using the Bandfit program provided by Digilab. The key criteria used to judge the accuracy of deconvolution were (a) a low root-mean-squared error (RMSE) between the original spectrum and the sum of deconvolved bands and (b) the uniformity of the half-widths of these bands (between 1620 and 1700 cm^{-1}) which, measured at the half-heights of the peaks, were between 4.6 and 5.4 cm^{-1}. Assignments of amide I′ bands to different secondary structure elements were based on previously described assignments (Susi & Byler, 1986; Surewicz et al., 1988).

Quasielastic Light Scattering. Room-temperature light scattering measurements were performed with a Malvern 4700 spectrometer equipped with a 5-W argon ion laser (Spectra Physics) maintained at a power of 250 mW. TP40 and PE40δcys samples, at approximately 1 mg/mL, were filtered through a 0.22-μm filter prior to analysis. Measurements were made at a scattering angle of 90°, and hydrodynamic diameters (D_h) were calculated from diffusion coefficients obtained from a cumulant analysis of autocorrelation functions using the Stokes–Einstein equation (Koppel, 1972).

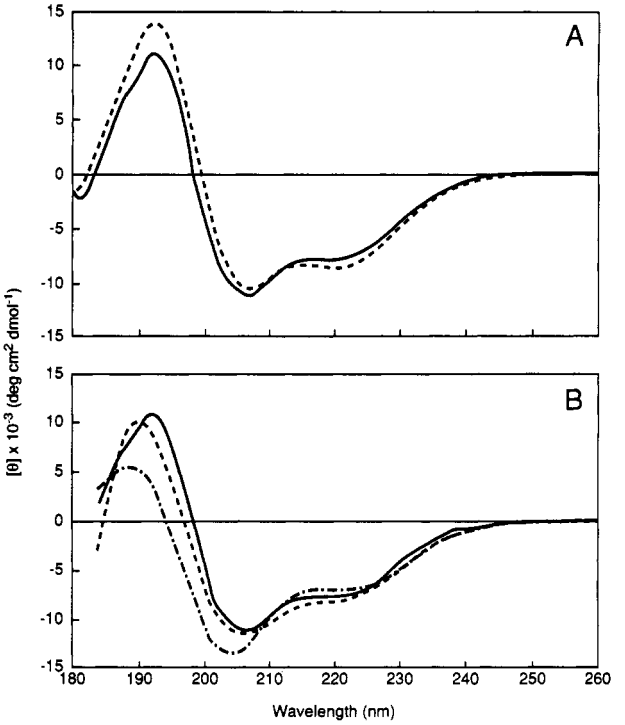

FIGURE 1: (A) Far-UV CD spectra of TP40 (—) and PE40δcys (- - -). Samples were prepared at a concentration of approximately 1 mg/mL in 100 mM sodium phosphate buffer at pH 7.2. Spectra were measured using a 0.1 mm path length cylindrical cuvette at 25 °C. (B) CD spectra of TP40 at pH 2.5 (- - -), 7.2 (—), and 11.4 (- · - · -). Experimental conditions were as in A.

Analytical Ultracentrifugation. Sedimentation equilibrium measurements were performed with a Beckman Optima XL-A analytical ultracentrifuge using rotor speeds of 10 000 and 15 000 rpm. Protein absorbance at a fixed wavelength was measured as a function of radial distance every few hours until superimposable traces were obtained at two consecutive time points, indicating that equilibrium had been established. Absorbance was monitored at 280 nm for TP40 and PE40δcys at concentrations of 0.1 and 0.25 mg/mL and at 295 nm for TP40 at 1.0 mg/mL. The temperature of the rotor was maintained at either 4 or 25 °C during each equilibrium experiment. Samples of TP40 at different pH values were prepared by dialyzing a pH 7.2 sample against buffer solutions of the desired pH. Protein concentrations less than 1 mg/mL were obtained by dilution in the appropriate buffer. The partial specific volumes of TP40 and PE40δcys were calculated from their known amino acid compositions. The data were analyzed by the Nonlin software package provided by the National Analytical Ultracentrifugation Facility of the University of Connecticut. Sedimentation velocity measurements were made at 20 °C at a rotor speed of 40 000 rpm. Data were analyzed by the dc/dt software provided by the National Analytical Ultracentrifugation Facility (University of Connecticut).

RESULTS

CD Spectra of TP40 and PE40δcys. The far-UV (184–260 nm) CD spectra of TP40 and its PE40δcys component were compared at pH 7.2 (Figure 1). The similarity of the two spectra suggests that the secondary structure of TP40 is dominated by its larger PE40δcys component. The CD spectrum of human TGF-α was measured under the same buffer and pH conditions as those used for TP40 (data not shown). If we assume that the CD of TGF-α was unaffected

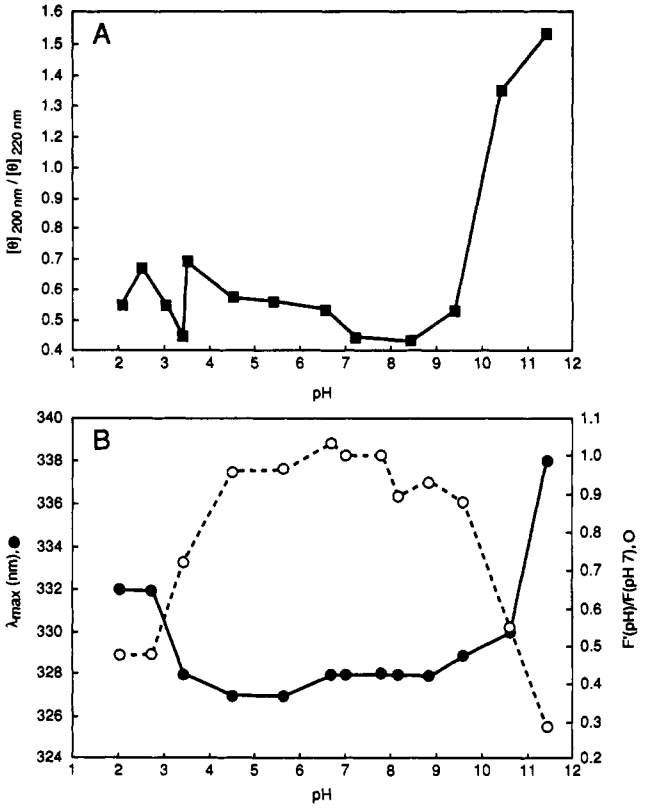

FIGURE 2: pH dependence of the structure of TP40 as monitored by CD and fluorescence spectroscopy. (A) Ratio of circular dichroism (ellipticity) at 200 nm to that at 220 nm as a function of pH. (B) Wavelength of maximum fluorescence (λ_{max}) as a function of pH. Measurements were made at 25 °C. Samples were excited at 280 nm. Excitation and emission bandpasses were 4 and 8 nm, respectively.

by its fusion with PE40δcys, the relative contributions of TGF-α to the ellipticities of TP40 at 206 and 220 nm are 14% and 3%, respectively. The secondary structure contents of TP40 and PE40δcys were estimated by the unconstrained variable selection method (Manavalan & Johnson, 1987). TP40 and PE40δcys were found to contain similar amounts of α-helix (23–28%), β-sheet (21–31%), turns (23–29%), and unordered structures.

pH Dependence of the CD Spectrum of TP40. The pH dependence of the CD spectrum of TP40 was examined over a pH range of 2.5–11.4. The spectra were similar between pH values of 5.0 and 9.0. Significantly different CD spectra were obtained above pH 10.0 and below pH 4.0. Spectra at pH 2.5, 7.2, and 11.4 are shown in Figure 1B. The spectrum at pH 11.4 manifests a blue shift of the 206-nm minimum to 202 nm accompanied by an increase in CD intensity, suggesting an increase in unordered structure. The structural change at these higher pH values is more clearly visualized when the ratio of the intensity at 200 nm to that at 220 nm is plotted as a function of pH (Figure 2A). The steep increase in this ratio with increasing pH above pH 9 suggests a major structural disruption (e.g., unfolding) of the protein. This ratio is much less sensitive to pH around and below neutrality. A considerable amount of secondary structure continues to be manifested in the CD spectra at low pH, although subtle changes relative to pH 7 are observed, e.g., a small blue shift of the ellipticity maximum near 195 nm and increased amplitude of the 206-nm minimum. The far-UV CD spectra (200–250 nm) of human TGF-α at pH 7.2 and 2.5 were virtually superimposable (data not shown).

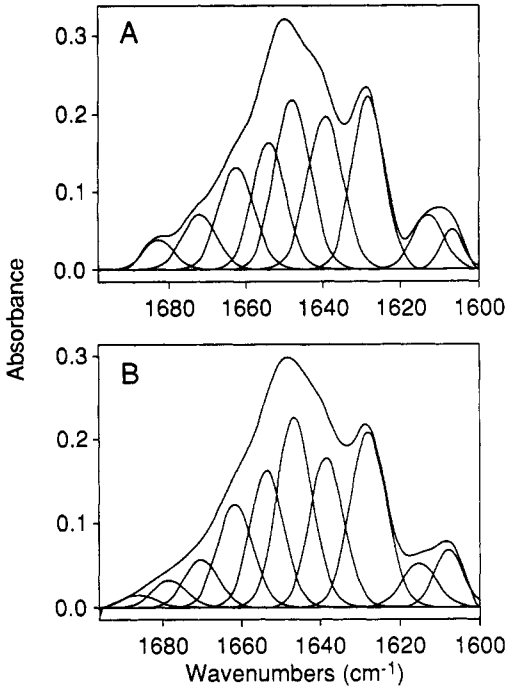

FIGURE 3: FTIR spectra of the amide I′ region of (A) TP40 and (B) PE40δcys. Experimental conditions are described under Methods. The partially deconvoluted spectrum and the fully deconvoluted bands are shown. Peak frequencies, bandwidths, and areas under these bands are listed in Table I.

pH Dependence of the Tryptophan Fluorescence of TP40. TP40 contains four tryptophan residues, all of which occur in the PE40δcys portion of the molecule. TGF-α contains no tryptophan. The tryptophan fluorescence of TP40 was measured as a function of pH in a 100 mM sodium phosphate buffer. Plots of the emission maximum (λ_{max}) and the relative fluorescence intensity at λ_{max} versus pH are shown in Figure 2B. The λ_{max} value remains nearly invariant (327–328 nm) between pH 3.4 and 8.8, but is increasingly red shifted with increasing pH above pH 8.8, reaching 338 nm at pH 11.4. The red shift of the fluorescence spectrum above pH 9 probably reflects partial unfolding of the protein as detected by CD measurements (Figure 2A). At pH values below 3, the λ_{max} is again red shifted relative to pH 7.2 to 332 nm. A plot of relative fluorescence intensity versus pH yields a bell-shaped curve with virtually constant fluorescence between pH 4 and 8. The half-maximal fluorescence change in the acid pH arm of this curve occurs at approximately pH 3.2. These data suggest that some increased solvent exposure of one or more tryptophan residues occurs below pH 4. These findings are similar, but not identical, to those of Jiang and London (1990), who observed a slightly blue-shifted fluorescence for PE between pH 3.7 and 5.4 and a red-shifted fluorescence below pH 3.7.

It should be noted that the tryptophan residues of TP40 do not appear to be fully solvent exposed even at pH 2 or 11.4, as indicated by the position of λ_{max}. Further red shift of the fluorescence spectrum, suggesting increased exposure of indole to solvent, is induced by guanidine hydrochloride (GuHCl). The approximate midpoint of the λ_{max} versus GuHCl concentration curve occurs at 1.8 M at pH 2.5 compared to 1.4 M at pH 7.2. The transition also appears broader (less cooperative) at pH 2.5 than at pH 7.2 (data not shown).

FTIR Spectra of TP40 and PE40δcys. The amide I′ regions of the TP40 and PE40δcys FTIR spectra are shown in Figure 3. The positions and widths of the absorption bands between 1620 and 1700 cm^{-1}, the relative areas under these bands, and

Table I: FTIR Amide I′ (1620–1700 cm^{-1}) Spectral Characteristics of TP40 and PE40δcys[a]

protein	peak frequency (cm^{-1})	band[b] half-width (cm^{-1})	relative peak area	assignment[c]
TP40	1628	4.8	0.20	β-strand
	1639	5.4	0.20	β-strand
	1648	5.3	0.22	unordered
	1654	5.0	0.15	α-helix
	1662	5.3	0.13	turn
	1672	5.3	0.07	turn or β-strand
	1683	4.6	0.03	turn
PE40δcys	1628	5.3	0.21	β-strand
	1638	5.0	0.17	β-strand
	1646	5.2	0.23	unordered
	1653	5.0	0.16	α-helix
	1662	5.2	0.12	turn
	1670	5.1	0.06	turn
	1678	5.0	0.03	β-strand
	1686	5.1	0.02	turn

[a] Measurements were made at ambient temperature using approximately 5 mg/mL TP40 and 6 mg/mL PE40δcys at pD = 7.2. [b] Half-width at half peak height. [c] Based on the assignments of Susi and Byler (1986). Because of overlap between a pair of adjacent bands, assignment to individual secondary structure contents in the 1640–1660 cm^{-1} region should be considered tentative. For example, the bands centered at 1648 and 1654 cm^{-1} (TP40) may both contain contributions from α-helix and unordered structures. Also, the 1639 cm^{-1} band may contain contributions from both β-sheet and unordered structure.

the assignments to different secondary structure types (Susi & Byler, 1986) are summarized in Table I. The close similarity between the TP40 and PE40δcys spectra is again consistent with PE40δcys being the principal contributor to the total secondary structure of TP40. The FTIR spectra suggest less α-helix and more β-sheet structure in TP40 and PE40δcys than were determined from CD. It should be noted, however, that there are fundamental differences between the methods used to analyze FTIR and CD spectra. Furthermore, uncertainties in amide I′ band assignments, especially around 1650 cm^{-1}, as well as extensive overlap between bands make accurate quantitation of secondary structure contents difficult, particularly for α-helix and unordered conformations (Bandekar & Krimm, 1980; Prestrelski et al., 1992). CD spectra, on the other hand, usually yield reliable estimates of α-helices, while estimates of β-sheets and turn structures are associated with larger margins of error (Johnson, 1990). The possibility of side-chain contribution was not taken into account in the analysis of either FTIR (Venyaminov & Kalnin, 1990) or CD (Manning, 1989) spectra.

TNS Binding to TP40 as a Function of pH. The binding of TNS to TP40 was measured as a function of pH by monitoring TNS fluorescence intensity and anisotropy at room temperature. TNS is known to bind to hydrophobic regions of many proteins (McClure & Edelman, 1966). While TNS shows only a weak fluorescence when free in aqueous solution, its fluorescence is strongly increased in nonpolar environments. The fluorescence of TNS is markedly enhanced in the presence of TP40 in a pH-dependent manner (Figure 4). The relative fluorescence intensity of TNS at pH 5 was approximately 3-fold higher than that at pH 7 in the presence of TP40. A much more dramatic increase in fluorescence intensity was observed when the pH was reduced to values below 4.0. The relative intensity at pH 3.0 was nearly 100-fold higher than that at pH 7.0. Thus, the extent of apparent exposure of hydrophobic surface is relatively slight until the pH is below 4. These results are consistent with the tryptophan fluorescence data described earlier. However, the greater sensitivity of TNS fluorescence allows detection of some exposure of

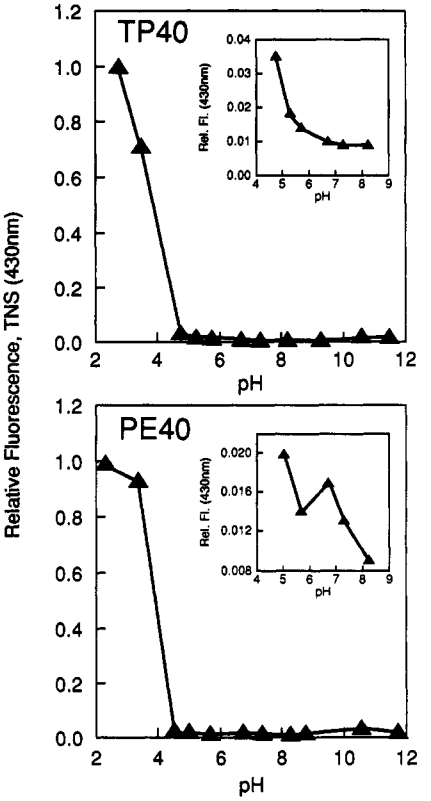

FIGURE 4: Low-pH-induced enhancement of TNS fluorescence in the presence of TP40 and PE40δcys. Solutions containing 22 μM TNS and 2 μM TP40 or 2 μM PE40δcys were excited at 315 nm. Fluorescence intensities at 430 nm (emission maximum) were normalized to the highest intensity observed at the lowest pH. The insets show a magnified view of a subset of the same data over a narrower pH range. Measurements were made at ca. 25 °C.

hydrophobic regions between pH 4 and 6. TNS fluorescence is also enhanced by PE40δcys in a pH-dependent fashion similar to that manifested by TP40 (Figure 4), suggesting that the hydrophobic regions of TP40 exposed by low pH occur predominantly in the PE40δcys portion of the conjugate protein. This conclusion is supported by our finding that TNS fluorescence is only slightly enhanced at low pH by human TGF-α. At pH 2.5, the fluorescence intensity (at 430 nm) of 22 μM TNS in the presence 2 μM TP40 is 700 times greater than that of a mixture of 22 μM TNS and 2 μM TGF-α.

Interaction of TP40 with Liposomes As Detected by Tryptophan Fluorescence. From the data reported above, it is apparent that at acidic pH a hydrophobic region in TP40 is exposed which does not cause a major perturbation of its secondary structure. To address whether this pH-induced structural change enables TP40 to associate with membranes, we investigated the effect of acidification on TP40–liposome interactions employing DSPC:DOPG REVs.

TP40 titrated with HCl in the presence of liposomes exhibited a gradual blue shift of its fluorescence spectrum (Figure 5A). This is in contrast to the low-pH-induced red-shift of the tryptophan fluorescence spectrum observed when TP40 alone was titrated with HCl in the absence of liposomes. Thus, at least one of TP40's tryptophan residues appears to be a part of a hydrophobic region which, at low pH, is exposed and available to interact with the liposome bilayer. This interaction results in one or more indole side chains experiencing a more apolar environment, resulting in the observed blue shift. It should be noted that, while the low-pH-induced red shift of TP40 fluorescence is not observed above pH 3.5, the blue shift of fluorescence in the presence of liposomes is

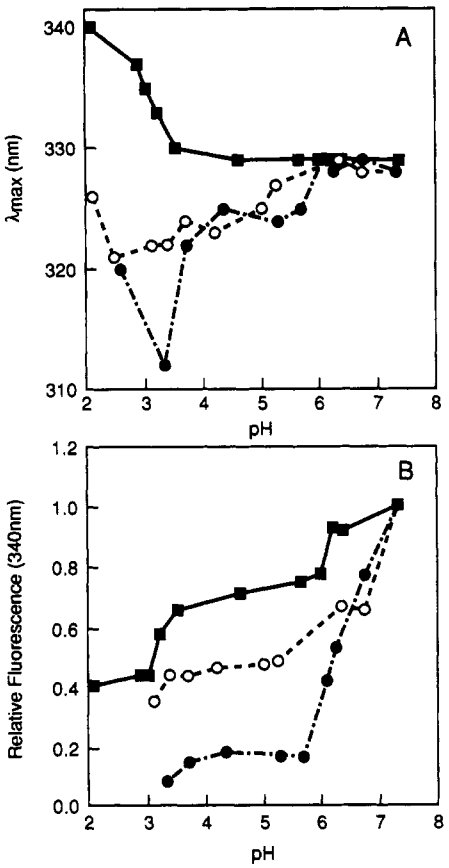

FIGURE 5: (A) Intrinsic tryptophan fluorescence emission maximum versus pH for TP40 alone (■), TP40 in the presence of 1:1 DSPC:DOPG REVs (○), and TP40 in the presence of 1:1 brominated DSPC:DOPG REVs (●). Samples containing 0.2 μM TP40 and 1.8 μM REVs in 10 mM sodium phosphate buffer (pH 7.4) were titrated with HCl directly in the cuvette. The wavelength of excitation was 280 nm. Fluorescence spectra were recorded at ca. 25 °C. (B) Relative intrinsic tryptophan fluorescence intensity monitored at 340 nm versus pH of TP40 alone (■), TP40 in the presence of 1:1 DSPC:DOPG REVs (○), and TP40 in the presence of 1:1 brominated DSPC:DOPG REVs (●). Conditions are the same as described in A.

apparent at pH 5.3 and below. The approximate midpoints of these transitions occur around pH 3.0 in the absence of liposomes and around pH 5 in the presence of DSPC:DOPG vesicles (disregarding the partial reversal of blue shift at pH 2.0). The negative charge of these vesicles might effectively lower the pH in the immediate environment of TP40, thus allowing the required structural transition to occur at a higher solution pH. A similar pH dependence of the tryptophan fluorescence spectrum of PE in the absence and presence of anionic vesicles has previously been reported (Jiang & London, 1990).

The interaction of TP40 with liposomes is confirmed by the observed quenching of TP40 tryptophan fluorescence by brominated DSPC:DOPG vesicles (Figure 5B). One or more tryptophan residues of the protein must be within interacting distance of the quenching bromide moiety present in the liposomes. This conclusion is based on the assumption that quenching is static rather than collisional. The dependence of the quenching on acidic pH and the presence of a much lower bromide concentration in the liposomes than that typically required for dynamic quenching support this assumption. The spectral blue shift induced by the liposomes was not reversed within 2 h, suggesting that upon interaction TP40 does not efficiently traverse the bilayer under the conditions of the experiment, although it may be partially entering the liposome. The observed red shift of tryptophan

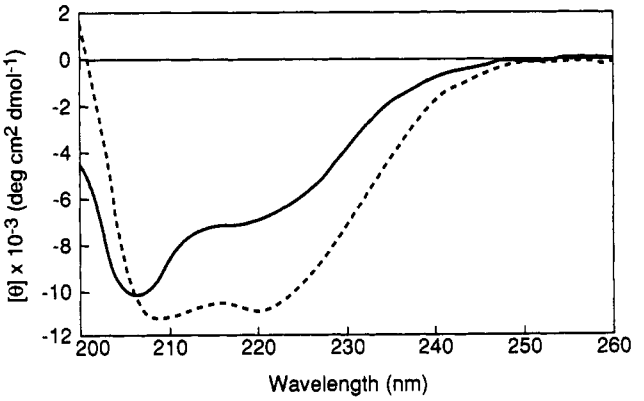

FIGURE 6: Circular dichroic spectra of TP40 in the presence of 1:1 DSPC:DOPG REVs at pH 7.4 (—) and pH 3.4 (- - -). TP40 and REVs (0.1 μm filtered) were each present at a concentration of approximately 0.24 μM in 10 mM sodium phosphate buffer, pH 7.4. The pH was adjusted in the cuvette with HCl. A path length of 1 cm was employed, and the temperature was 23 °C.

fluorescence at pH 2.1, compared to pH 2.4, in the presence of both vesicle preparations may suggest an additional conformational change in TP40, the nature of which is unclear. Neutral liposomes of equimolar egg PC:cholesterol failed to manifest the spectral changes seen with the negatively charged vesicles.

CD Spectral Change of TP40 upon Interaction with Liposomes. The interaction of DSPC:DOPG REVs with TP40 at low pH appears to be accompanied by induction of helicity in the protein as judged by CD (Figure 6). At pH 3.4 in the presence of these vesicles, a distinct minimum at 222 nm emerged and the 206-nm minimum was shifted to 208 nm. The mean residue ellipticity at 222 nm was increased from −6577 deg·cm^2 dmol^{-1} at pH 7.2 to −10 570 deg·cm^2 dmol^{-1} at pH 3.4, which corresponds to an increase in the percentage contribution of α-helix from approximately 22% to 35% (Chen et al., 1972).

Distortion of the CD spectra of proteins in liposomes may be caused by both differential light scattering and absorption flattening (Mao & Wallace, 1984). Potential light scattering artifacts were corrected by subtracting the CD signal of blank liposomes at equivalent pH. The absence of any spurious band in the optically transparent regions (e.g., above 240 nm) of the CD spectrum (Figure 6) suggests that differential scattering was not a significant problem. Absorption flattening, which may occur when the UV-absorbing protein molecules are tightly packed in vesicles, would normally reduce the absorption and, consequently, the magnitude of CD relative to a protein solution in which the molecules are uniformly dispersed. For a given concentration of TP40, the presence of DSPC:DOPG REVs did not reduce the CD signal at any wavelength at either pH 7.4 or 3.4. Therefore, we assume that the CD spectra presented in Figure 6 exhibit little or no absorption flattening.

Hydrodynamic Size of TP40 as a Function of pH. The pH dependence of the hydrodynamic size of TP40 was determined by QLS measurements over a pH range of 2.0–11.4 (Table II). The hydrodynamic diameter (D_h) was smallest (ca. 8 nm) around neutral pH and increased dramatically below pH 5.5. The theoretically calculated value of D_h for a spherical molecule of TP40 is 8.4 nm, assuming a partial specific volume of 0.728 cm^3 g^{-1} (based on the amino acid composition of TP40) and a hydration volume of 0.35 cm^3 per cm^3 of the protein. Reproducible QLS measurements of D_h between pH 4.0 and 5.5 were not obtained because of varying extents of

Table II: *Z*-Average Mean Hydrodynamic Diameter (D_h) of TP40 as a Function of pH[a]

pH	D_h (nm)	polydispersity index (nm)
2.00	17.6	0.183
2.96	16.7	0.163
3.59	24.8	0.120
4.36	>100	0.128
5.51	9.5[b]	0.604[b]
6.34	8.7	0.292
7.20	8.2	0.282
7.78	9.7	0.330
8.66	9.1	0.290
9.93	8.7	0.279
10.9	10.3	0.266

[a] Measurements were made at 25 °C on TP40 solutions at a concentration of approximately 1 mg/mL. Samples at different pH values were prepared by dialyzing a 1 mg/mL solution at pH 7 against 100 mM phosphate buffer of the desired pH. [b] A small amount (~3%) of a larger sized material (D_h range of 35–48 nm) was detected, which accounts for the relatively high polydispersity index.

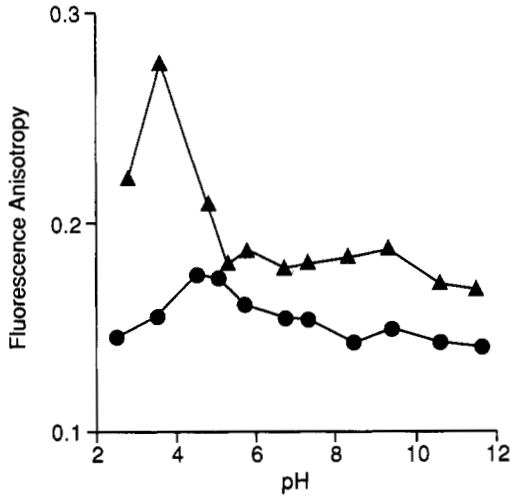

FIGURE 7: Steady-state tryptophan fluorescence anisotropy of TP40 and PE40δcys measured at 25 °C as a function of pH. Samples containing 1 mg/mL protein were excited with polarized light at 300 nm. Parallel and perpendicular components of polarized emission were monitored at 350 nm. Excitation and emission bandpasses of 8 nm were used.

aggregation, presumably due to the proximity of these pH values to the isoelectric pH (4.9) of TP40. The presence of even a small amount of a large aggregate can skew the mean D_h toward a spuriously high value. Initial measurements at pH 5.5 yielded values similar to those at pH 7.2. However, a slow increase of D_h was observed over a period of several hours (at 25 °C). Between pH 2 and 4, TP40 appeared to be relatively homogeneous in size, as manifested in the smaller values of the cumulant polydispersity index. The pH–size profile for PE40δcys was found to be similar to that of TP40 exhibiting increased D_h at acidic pH (data not shown).

Fluorescence Anisotropy. The intrinsic tryptophan fluorescence anisotropy (r) of TP40 measured in the steady state at 25 °C remained approximately constant between pH 5.3 and 9.3. It then increased with decreasing pH below pH 5.3 and reached a maximum at pH 3.5 (Figure 7). The anisotropy at pH 2.7 was less than that at pH 3.5 but significantly higher than that at pH 7.3. While this profile is consistent with low-pH-induced self-association, environmental perturbations around the tryptophan residues could cause increased or decreased local mobility, resulting in altered anisotropy. It should be noted that the average tryptophan lifetime in TP40 at pH 3.5 is shorter than that at pH 7.2 (Table III), which could partially account for the higher anisotropy at the lower

Table III: Tryptophan Fluorescence Lifetime (τ) of TP40 as a Function of pH[a]

pH	τ_1 (ns)	τ_2 (ns)	f_1[b]	f_2[b]	τ_{av}[c] (ns)	χ^2
3.5	5.7	1.6	0.70	0.30	4.5	4.1
6.0	6.6	1.9	0.79	0.21	5.6	6.0
7.2	6.3	1.8	0.80	0.20	5.4	5.2
8.0	6.7	2.0	0.74	0.20	5.5	5.8
11.6	4.3	1.1	0.57	0.43	2.9	3.6

[a] A two-component least-squares analysis provided the best fit to the observed phase shift and demodulation data, as judged by the reduced χ^2 and distribution of residuals. Standard deviations of 0.4° in phase angle and 0.008 in modulation ratios were assumed, on the basis of the precision of the measurements. [b] f_1 and f_2 represent the fractional contributions of the two components to the total fluorescence intensity, decaying with lifetimes τ_1 and τ_2, respectively. [c] $\tau_{av} = \tau_1 f_1 + \tau_2 f_2$.

pH. The decrease in anisotropy above pH 10, despite an apparent decrease in the mean lifetime relative to pH 7 (Table III), is probably due to increased mobility of one or more contributing tryptophans resulting from unfolding.

The pH–anisotropy profile for PE40δcys was qualitatively similar to that of TP40. However, anisotropy values were somewhat less. This could be due to higher motional freedom of one or more tryptophan residues, possibly near the TGF-α conjugation site, in PE40δcys relative to TP40. The slightly smaller molecular size of PE40δcys could account for a further small decrease in anisotropy.

Tryptophan Fluorescence Lifetime of TP40 as a Function of pH. The tryptophan fluorescence lifetimes of TP40 at different pH values from 3.5 to 11.6 are listed in Table III. The phase shift and demodulation data were analyzed as a single exponential and as a sum of two or three exponentials. A two-component analysis provided the best fit. The most significant difference, relative to pH 7.2, was observed at pH 11.6. The fractional contribution of the longer lifetime component to the total fluorescence intensity and the average lifetime were appreciably smaller at high pH. This may be a result of the conformational change that was reflected in CD and steady-state fluorescence measurements. The average lifetime at pH 3.5 was also smaller than that at pH 7.2.

Equilibrium Sedimentation. Equilibrium sedimentation measurements made at 1 mg/mL protein at 20 and 25 °C also revealed self-association at pH 2.5, while no evidence for associated states was apparent in the pH range 5.3–7.2 (Table IV). A process of slow aggregation, accompanied by loss of protein from solution, was observed at pH 3.9 during the course of centrifugation at 15 000 rpm. This phenomenon was not observed when measurements were made on a pH 3.9 sample at 4 °C using 0.25 mg/mL TP40. These observations suggest that aggregation at this pH is facilitated by higher concentrations and temperatures. A high degree of self-association was, however, observed even at 4 °C for solutions at pH 2.5 and 3.2 at protein concentrations of 0.1, 0.25, and 1 mg/mL. Addition of 22 μM TNS to 2.2 μM TP40 (conditions of fluorescence experiment) at pH 2.5 did not change the state of association.

Velocity Sedimentation. Between pH 5.3 and 7.2, nearly invariant sedimentation coefficients, 2.50 ± 0.05, were obtained for 1 mg/mL TP40 at 20 °C. At pH 2.5, the data were best fit by two components with sedimentation coefficients of 2.5 S and 10.0 S. These data are consistent with equilibrium sedimentation data which suggested the presence of a predominantly monomeric species between pH 5.3 and 7.2 and a high degree of self-association in solution at pH 2.5.

pH Dependence of Bioactivity. TP40 samples incubated at different pH values ranging from 3.4 to 11.5 were assayed for

Table IV: Estimates of Molecular Weights (MW) and Sedimentation Coefficients (S) of TP40 as a Function of pH As Determined by Equilibrium Sedimentation and Velocity Sedimentation Measurements

pH	best-fit model[a]	MW[a]	$S_{20°C}$[b]
2.52	single species[c]	443 090	2.42, 10.00
3.93[d]		not determined (insoluble material)	not determined
5.25	single species	46 307	2.55
5.44	single species	42 004	2.53
5.65	single species	41 158	2.46
7.04	single species	45 085	2.51

[a] Equilibrium measurements were performed with 1 mg/mL TP40 solutions at approximately 25 °C. Data from both 10 000 and 15 000 rpm centrifugations were used in the Nonlin analysis to generate the best-fit model and the MW. [b] Velocity measurements were made on 1 mg/mL TP40 solutions at 20 °C at a rotor speed of 40 000 rpm. Results are expressed in Svedberg units (S). [c] Although the best fit was obtained assuming a single species of approximately 10 times the MW of a monomer, almost equally good fits resulted assuming equilibrium between multimers of different sizes. Measurements at 4 °C yielded a monomer–hexamer equilibrium as the best fit for TP40 solutions (0.25 mg/mL) at pH 2.5 and 3.2. Velocity sedimentation data could also be fit to two components with widely different S values. [d] Precipitation of TP40 from solution occurred during centrifugation. At 4 °C, using 0.25 mg/mL TP40, a single species with a MW of 47 945 was obtained as the best fit.

Table V: In Vitro Cell-Kill Bioactivity of TP40 Samples Incubated at Different pH Values[a]

incubation pH	relative potency[b]	95% confidence interval
3.4	0.99	0.92–1.08
5.5	0.83	0.81–0.85
7.2	0.95	0.91–0.99
8.2	0.87	0.81–0.93
11.5	0.20	0.18–0.24

[a] Samples incubated at 5 °C in 100 mM sodium phosphate buffers at the indicated pH were transferred and diluted into the assay medium at 37 °C, pH 7.4. [b] Relative potency represents the ratio of EC_{50} of the assay standard to that of the sample, where EC_{50} is the concentration of TP40 at which 50% cell survival is observed. Typical EC_{50} values were 35–50 pM under these assay conditions. The assay standard was structurally well characterized, stored at −70 °C, and fully bioactive.

in vitro bioactivity in a cell-kill assay. The relative potencies, measured against a fully active assay standard at pH 7.2, are indicated in Table V. The bioactivity of TP40 is approximately the same over a pH range of 3.4–8.2, when allowance is made for the large standard deviation (ca. 27%) inherent in the assay. Because the pH of the assay medium is 7.4, the full bioactivity observed for the pH 3.4 sample suggests that any potentially deleterious effect of low pH, e.g., aggregation, on activity is reversed by returning the sample pH to neutrality. A major loss of activity was, however, observed for a TP40 sample incubated at pH 11.5. This result suggests that the structural change observed at this pH by CD is irreversible.

DISCUSSION

Conformation(s) of TP40 at Low pH. The role of a low-pH-induced conformational change in PE in translocation across the endosomal membrane has been previously described (Zalman & Wisnieski, 1985; Sandvig & Moskaug, J. L., 1987; Farahbakhsh & Wisnieski, 1989; Jiang & London, 1990). Changes in intrinsic tryptophan fluorescence, binding of the hydrophobic fluorescence probes ANS and TNS, and susceptibility to proteolysis have been used to examine the effect of acidification on the structure and membrane interaction of PE. Two forms of PE, each distinct from its pH 7 conformation, have been proposed to exist at acidic pH (Farahbakhsh & Wisnieski, 1989; Jiang & London, 1990). Between pH 3.7 and 5.4, a folded conformation manifesting a slightly blue-shifted tryptophan fluorescence relative to that at pH 7 has been described. At pH values below pH 3.7, a different state, resembling that of the unfolded protein with "strong hydrophobicity", has been postulated by the same authors. In the case of TP40 we have observed a very slight exposure of apolar regions under weakly acidic conditions as judged by a small enhancement in TNS fluorescence and lack of a red shift in tryptophan emission. Below pH 3.5, a large increase in TNS binding and a significant red shift of tryptophan fluorescence are consistent with marked exposure of hydrophobic domains to solvent. This does not appear, however, to be a fully unfolded state as judged by CD, fluorescence, and the induction of further spectroscopic changes by guanidine hydrochloride. Furthermore, the fluorescence λ_{max} for a pH 11.4 TP40 sample, which appears to be at least partially unfolded on the basis of its CD spectrum, is 338 nm while that for a pH 2.5 sample is only 332 nm.

The Nature of the Low-pH State. The marked enhancement of TNS binding to TP40 and PE40δcys, coupled with the lack of a major CD spectral change at pH values <4, raises the interesting question of whether a "molten globule" type of structure might be formed. The molten globule state of a protein is characterized by extensive secondary structure content, but a substantial loss of tertiary structure while maintaining a compact form. Such states are found at low pH and high anion concentration and at subdenaturing levels of structural perturbants. They are thought to be early intermediates in the folding pathways of many proteins (Kuwajima, 1989; Dobson, 1992). Interpretation of the low-pH TNS binding data for TP40 and PE40δcys is complicated by aggregation of these proteins. However, aggregation via intermolecular nonpolar interactions is also a commonly observed characteristic of molten globule states (Christensen & Pain, 1991). Although the tryptophan fluorescence spectra of TP40 and PE40δcys at pH 2 are red shifted relative to those at pH 7, the average solvent exposure of these tryptophan residues appears to be only partial even at this low pH. This is apparently inconsistent with typical molten globule states, which usually display extensive loss of tertiary structure leading to an almost total exposure of indole side chains to solvent (Baldwin, 1991). However, low-pH-induced folding intermediates with apparently buried tryptophan residues have been observed, e.g., β-lactamase in 0.5 M KCl (Goto & Fink, 1989). Solvent exposure of tryptophans may be masked by aggregation if the protein–protein interface contains tryptophan residues. The possibility of the involvement of a molten globule structure in the translocation of PE has been suggested (Jiang & London, 1990), although the secondary structure of the intact toxin has not been examined by CD below pH 4 (Farahbakhsh et al., 1987).

Secondary Structure of TP40. The secondary structure of TP40 is largely dominated by that of PE40δcys, as judged by their very similar CD and FTIR spectra. The secondary structure contents of TP40 and PE40δcys estimated from these spectra are virtually indistinguishable. This is not surprising since PE40δcys constitutes approximately 89% by mass of the TP40 molecule. The percentage of α-helix calculated from the CD spectrum of TP40 (and PE40δcys) is consistent with crystal structure data on PE (Allured et al., 1986), which shows six consecutive helices between residues 253 and 354 of domain II. Domain Ib of PE, containing residues 365–404, has several β-strands. This domain is present in PE40δcys and is probably the major source of the β-sheet structure suggested by the CD and FTIR spectra of TP40. The carboxy

terminal domain of PE (domain III), which also occurs in PE40δcys, has a less ordered structure than domains II and Ib. The CD spectrum of PE has been reported (Farahbakhsh et al., 1987). In general, this spectrum reflects significant contributions from α-helix and β-sheet structures. The major difference between the CD spectra of PE and TP40 (or PE40δcys) is that the former manifests a broad minimum between 205 and 220 nm, as opposed to the distinct 206-nm minimum accompanied by a shoulder around 220 nm that we observed for the latter. No major change in the secondary structure of PE was manifested in the CD spectra when the pH was dropped from 7.7 to 4.0 (Farabakhsh et al., 1987).

Primary Structure and Translocation Mechanism. A major difference between the primary structures of domains II and III of PE and their counterparts in PE40δcys is the presence of disulfide bonds in the former and lack of cysteines or cystines in the latter. The translocation of PE into the cytosol is believed to be preceded by (1) proteolytic cleavage near Arg-279, which occurs in a disulfide loop bounded by Cys-265 and Cys-287, and (2) reduction of this disulfide bond. The resultant 37-kDa C-terminal fragment is then thought to translocate across the endosomal membrane into the cytosol where ADP-ribosylation occurs (Ogata et al., 1990). A hybrid protein containing only this fragment of PE (PE37), which lacks the Cys-265–Cys-278 loop, conjugated to TGF-α has been found to be highly cytotoxic against EGFr-rich cell lines (Theuer et al., 1992). In a recently proposed model, the transfer of this 37-kDa fragment to the endoplasmic reticulum by a trans-Golgi mechanism has been proposed (Pastan et al., 1992). If the mechanism postulated in this model is operative, the low-pH-induced conformational change of PE would facilitate exposure of the proteolytic site at the Arg-279–Gly-280 bond to an undefined cellular protease. It is proposed that cleavage of this bond followed by reduction of the Cys-265–Cys-287 disulfide bond generates the "active" PE fragment (Ogata et al., 1990). This disulfide loop is absent in TP40. It is conceivable that proteolytic clipping at the Arg-279–Gly-280 bond may still occur to generate an active C-terminal fragment. In any event, translocation of TP40 must occur since this conjugate has high cytotoxicity against A431 and other EGFr-containing cell lines (Edwards et al., 1989).

TP40 Interaction with Anionic Liposomes and Relevance to Translocation. Induction of a spectral blue shift of TP40 fluorescence by anionic liposomes and quenching of fluorescence by brominated DSPC:DOPG vesicles occur at pH values close to endosomal pH. Similar observations have been reported for PE (Jiang & London, 1990). Furthermore, interaction of TP40 with negatively charged vesicles at acidic pH is also associated with a transition of TP40 structure to a more helical form, which is not induced by low pH alone in the absence of liposomes. Induction of helical structure in the PhoE signal peptide by anionic phospholipids has been observed and implicated in translocation of this peptide across the plasma membrane (Keller et al., 1992).

Conclusions. Our findings suggest that TP40, an engineered fusion protein, retains the structural features that are necessary for carrying out its complex functions leading to antitumor activity. Binding to EGFr, a property that resides in the TGF-α portion of this chimeric protein, as well as in vitro ADP-ribosylation activity and cytoxicity were demonstrated earlier (Edwards et al., 1989; Heimbrook et al., 1990). We have now shown that the structural flexibility required for pH-dependent translocation is also maintained. The structural changes of TP40 that we observe at low pH, namely, exposure of apolar regions, interaction with anionic liposomes and increased helicity induced by this interaction, are consistent with a direct role for an acidic pH-mediated conformational change in translocation of the protein across the endosomal membrane. In this conformation, the secondary structure of TP40 appears to be highly ordered and the tertiary structure partially maintained. The compactness of TP40 itself at acidic pH relative to the native structure at pH 7 could not be assessed because of self-association.

ACKNOWLEDGMENT

We are indebted to Dr. Shigeko Yamazaki for providing us with purified TP40 and PE40δcys and to Dr. Donald O'Keefe for analyzing the purity of protein preparations. Mr. James A. Ryan's help in the analysis of FTIR data is gratefully acknowledged. We thank Dr. David C. Heimbrook for helpful discussions.

REFERENCES

Allured, V., Collier, R. J., Carroll, S. F., & McKay, D. B. (1986) *Proc. Natl. Acad. Sci. U.S.A. 83*, 1320–1324.

Baldwin, R. L. (1991) *Chemtracts: Biochem. Mol. Biol. 2*, 379–389.

Banekar, J., & Krimm, S. (1988) *Biopolymers 27*, 909–921.

Blewitt, M. G., Chung, L. A., & London, E. (1985) *Biochemistry 24*, 5458–5464.

Chaudhury, V. K., FitzGerald, D. J., Adhya, S., & Pastan, I. (1987) *Proc. Natl. Acad. Sci. U.S.A. 84*, 4538–4542.

Chen, Y.-H., Yang, J. T., & Martinez, H. M. (1972) *Biochemistry 11*, 4120–4131.

Christensen, H., & Pain, R. H. (1991) *Eur. Biophys. J. 19*, 221–229.

Collier, R. J. (1975) *Bacteriol. Rev. 39*, 54–85.

Collins, C. M., & Collier, R. J. (1987) in *Membrane-Mediated Cytotoxicity* (Bonavide, B., & Collier, R. J., Eds.) Liss, New York.

Dobson, C. M. (1992) *Curr. Opin. Struct. Biol. 2*, 6–12.

Draper, R. K., & Simon, M. J. (1980) *J. Cell Biol. 87*, 849–854.

Edwards, G. M., DeFeo-Jones, D., Tai, J. Y., Vuocolo, G. A., Patrick, D. R., Heimbrook, D. C., & Oliff, A. (1989) *Mol. Cell. Biol. 9*, 2860–2867.

Farahbakhsh, Z. T., & Wisnieski, B. J. (1989) *Biochemistry 28*, 580–585.

Farahbakhsh, Z. T., Baldwin, R. L., & Wisnieski, B. J. (1987) *J. Biol. Chem. 262*, 2256–2261.

FitzGerald, D. J., Morris, R. E., & Saelinger, C. B. (1980) *Cell 21*, 867–873.

Goto, Y., & Fink, A. L. (1989) *Biochemistry 28*, 945–952.

Heimbrook, D. C., Stirdivant, S. M., Ahern, J. D., Balishin, N. L., Patrick, D. R., Edwards, G. M., DeFeo-Jones, D., FitzGerald, D. J., Pastan, I., & Oliff, A. (1990) *Proc. Natl. Acad. Sci. U.S.A. 87*, 4697–4701.

Iglewski, B. H., & Kabat, D. (1975) *Proc. Natl. Acad. Sci. U.S.A. 72*, 2284–2288.

Jiang, J. X., & London, E. (1990) *J. Biol. Chem. 265*, 8636–8641.

Johnson, W. C., Jr. (1990) *Proteins: Struct. Funct. Genet. 3*, 53–59.

Kauppinen, J. K., Moffatt, D. J., Mantsch, H. H., & Cameron, D. C. (1981) *Appl. Spectrosc. 35*, 271–227.

Keller, R. C. A., Killian, J. A., & Kruijff, B. D. (1992) *Biochemistry 31*, 1672–1677.

Kline, T. P., Brown, F. K., Brown, S. C., Jeffs, P. W., Kopple, K. D., & Mueller, L. (1990) *Biochemistry 29*, 7805–7813.

Koppel, D. E. (1972) *J. Chem. Phys. 57*, 4814–4820.

Kounnas, M. Z., Morris, R. E., Thompson, M. R., FitzGerald, D. J., Strickland, D. K., & Saelinger, C. B. (1992) *J. Biol. Chem. 267*, 12420–12423.

Kuwajima, K. (1989) *Proteins: Struct. Funct. Genet. 6*, 87–103.

Lakowicz, J. R., Laczko, G., Cherek, H., Gratton, E., & Limkeman, M. (1984) *Biophys. J. 46*, 463–477.
Lee, D. C., Rose, T. M., Webb, N. R., & Todaro, G. J. (1985) *Nature 313*, 489–491.
Mach, H., Middaugh, C. R., & Lewis, R. V. (1992) *Anal. Biochem. 200*, 74–80.
Manavalan, P., & Johnson, W. C., Jr. (1987) *Anal. Biochem. 167*, 76–85.
Manning, M. C. (1989) *J. Pharm. Biomed. Anal. 7*, 1103–1119.
Mao, D., & Wallace, B. A. (1984) *Biochemistry 23*, 2667–2673.
Marquardt, H., Hunkapiller, M. W., Hood, L. E., & Todaro, G. J. (1983) *Science 223*, 1079–1082.
Massague, J. (1983) *J. Biol. Chem. 258*, 13614–13620.
McClure, W. O., & Edelman, G. M. (1966) *Biochemistry 5*, 1908–1918.
Morris, R. E., Gerstein, A. S., Bonventre, P. F., & Saelinger, C. B. (1985) *Infect. Immun. 40*, 806–811.
Ogata, M., Chaudhuri, V. K., Pastan, I., & FitzGerald, D. J. (1990) *J. Biol. Chem. 265*, 20678–20685.
Pastan, I., & FitzGerald, D. (1989) *J. Biol. Chem. 264*, 15157–15160.
Pastan, I., & FitzGerald, D. (1991) *Science 254*, 1173–1177.
Pastan, I., Chaudhury, V., & FitzGerald, D. (1992) *Annu. Rev. Biochem. 61*, 331–354.
Prestrelski, S. J., Arakawa, T., Wu, C.-S. C., O'Neil, K. D., Westcott, K. R., & Narhi, L. O. (1992) *J. Biol. Chem. 267*, 319–322.
Sandvig, K., & Olsnes, S. (1980) *J. Cell Biol. 87*, 828–832.
Sandvig, K., & Moskaug, J. O. (1987) *Biochem. J. 245*, 899–901.
Surewicz, W. K., & Mantsch, H. H. (1988) *Biochim. Biophys. Acta 952*, 115–130.
Susi, H., & Byler, D. M. (1986) *Methods Enzymol. 130*, 290–311.
Szoka, F., Jr., & Papahadjopoulos, D. (1978) *Proc. Natl. Acad. Sci. U.S.A. 75*, 4194–4198.
Theuer, C. P., FitzGerald, D. J., & Pastan, I. (1992) *J. Biol. Chem. 267*, 16872–16877.
Venyaminov, S. Y., & Kalnin, N. N. (1990) *Biopolymers 30*, 1243–1257.
Von Hoff, D. D., Marshall, M. H., Heimbrook, D. C., Stirdivant, S. M., Ahern, J. D., Herbert, W. K., Maigetter, R. Z., & Oliff, A. (1992) *Invest. New Drugs 10*, 17–22.
Winkler, M. E., Bringman, T., & Marks, B. J. (1986) *J. Biol. Chem. 261*, 13838–13843.
Zalman, L. S., & Wisnieski, B. J. (1985) *Infect. Immun. 50*, 630–635.